Proceedings of the ASME 2018 37th International
Conference on Ocean, Offshore and Arctic Engineering
OMAE2018
June 17-22, 2018, Madrid, Spain

OMAE2018-78368

FULLY-COUPLED AERO-HYDRODYNAMIC SIMULATION OF FLOATING OFFSHORE WIND TURBINES BY DIFFERENT SIMULATION METHODS

Ping Cheng
Collaborative Innovation Center for Advanced Ship and Deep-Sea Exploration
State Key Laboratory of Ocean Engineering
School of Naval Architecture, Ocean and Civil Engineering
Shanghai Jiao Tong University
Shanghai, 200240, China

Decheng Wan*
Collaborative Innovation Center for Advanced Ship and Deep-Sea Exploration
State Key Laboratory of Ocean Engineering
School of Naval Architecture, Ocean and Civil Engineering
Shanghai Jiao Tong University
Shanghai, 200240, China
*Corresponding author: dcwan@sjtu.edu.cn

ABSTRACT

To accurately predict the critical loads due to wind and wave is one of the common challenges in designing a floating offshore wind turbine (FOWT). The fully-coupled aero-hydrodynamic simulation of a floating offshore wind turbine, the NREL-5MW baseline wind turbine mounted on a semi-submersible floating platform, is conducted with two methods. Firstly, the in-house code naoe-FOAM-os-SJTU, which is developed on the open source platform OpenFOAM and coupled with the overset grid technique, is employed for the directly CFD computations. And another in-house code FOWT-UALM-SJTU developed by coupling the unsteady actuator line model (UALM) with naoe-FOAM-SJTU is also utilized for coupling simulations. In both models, the three-dimensional Reynolds Averaged Navier-Stokes (RANS) equations are solved with the turbulence model k-ω SST, and the Pressure-Implicit with Splitting of Operations (PISO) algorithm is applied to solve the pressure-velocity coupling equations.

Both two solvers provide reasonable results of main aerodynamic loads as well as the main hydrodynamic forces. The FOWT-UALM-SJTU solver achieves better computational efficiency by simplifying the blade structure as actuator line models, while the naoe-FOAM-os-SJTU solver provides more accurate detailed flow information near the turbine blades.

Keywords: Fully-coupled aero-hydrodynamic simulation; floating offshore wind turbine (FOWT); overset grid technique; unsteady actuator line model (UALM)

INTRODUCTION

The renewable wind energy represents a potential to resolve the energy crisis and environment pollution problem, especially for coastal countries with enormous ocean wind energy resource [1]. In recent years, floating offshore wind turbines (FOWT) have stood out and attracted more attention. The first multi-megawatt FOWT in the world was installed at the west coast of Norway in June 2009 [2]. Since then, more FOWTs have been emerged and served for coastal cities [3]. However, designing FOWT system is still a quite challenging task due to the complicated structure, the complex environmental loading and the coupling effects [4].

As an indispensable tool for research, model test plays an important role in study on FOWT. Model tests including intermediate-scale models monitored in offshore water areas [5] and scaled-down models tested in wave basin and wind tunnel [6-7] could provide more intuitionistic and practical data for further study. However, there still underlies a problem that the Froude scaling law and the Reynolds similarity law cannot be guaranteed at the same time, which makes the model test data less valuable in FOWT designing.

The numerical methods successfully avoid this scale-effect by conducting simulations with full-scale models, which is also much more economical than experimental tests. Recently, fully coupled aero-hydrodynamic simulations of FOWTs have been achieved under combined wind-wave conditions, the aerodynamics of wind turbine and the hydrodynamics of floating platform are analyzed, and the coupling effects are studied. Based on blade element momentum (BEM) method and potential flow theory, The National Renewable Energy Laboratory (NREL) developed a fully coupled aero-hydroservo-elastic tool named FAST [8] to implement the coupled simulation of FOWTs. However, developed based on potential flow and BEM theory, the FAST solver fails to model the flow viscous effect directly by solving the viscous N-S equations, which restricts its usage for more accurate predictions. In early studies, most numerical tools for coupling simulation of FOWT are developed based on BEM method, such as HAWC2, 3Dfloat, etc. [9]. As is known, BEM is an empirical method with various correction models (such as Glauert correction, skewed wake correction, etc.), some researchers [10] suggested that the BEM is still questionable in unsteady aerodynamic prediction for FOWTS.

Thanks to the rapid development of compute technology, more and more studies on fully coupled analysis of FOWTs have been conducted with CFD method. Tran [11-12] studied the impact of platform motions on unsteady aerodynamic performances of a wind turbine by setting periodic surging, pitching and yawing motions of the supporting platform. And the fully coupled aero-hydrodynamic analysis of a semi-submersible FOWT was then conducted using a dynamic fluid body interaction approach [13]. Based on OpenFOAM package, Liu [14] established a fully coupled CFD analysis tool for FOWTs and studied the coupling effect of the OC4 DeepCWind semi-submersible FOWT.

Based on the open source CFD platform OpenFOAM, our research team developed the CFD solver naoe-FOAM-SJTU to investigate hydrodynamic problems in the field of ship and ocean engineering. By introducing the unsteady actuator line model (UALM) [15] into OpenFOAM for aerodynamic simulation and combining with naoe-FOAM-SJTU solver, the fully coupled aero-hydrodynamic model for simulation of a floating offshore wind turbine is established, which is named the FOWT-UALM-SJTU solver [16]. As the UALM represents an approximate method in which the actual blades are simplified as a series of actuator elements, the FOWT-UALM-SJTU solver achieves higher computational efficiency. On the other hand, the absence of accurate expression of the blades surface with refined mesh leads to lack of detailed flow information near blades, which plays critical role in deeply mechanism research. Thus, the in-house naoe-FOAM-os-SJTU solver is employed to conduct direct CFD simulation of the FOWT.

NUMERICAL METHOD

Governing Equations

Both solvers are established based on the open source CFD platform OpenFOAM, and the two-phase three-dimensional (3D) Reynolds-Averaged Navier-Stokes (RANS) equations for transient, incompressible and viscous Newtonian fluid are employed, containing the continuity and momentum equations:

$$\nabla \cdot \mathbf{U} = 0 \tag{1}$$

$$\frac{\partial(\rho \mathbf{U})}{\partial t} + \nabla \cdot (\rho(\mathbf{U} - \mathbf{U}_g))\mathbf{U} = -\nabla p_d - \mathbf{g} \cdot \mathbf{x}\nabla\rho + \nabla \cdot (\mu_{eff}\nabla \mathbf{U}) + (\nabla \mathbf{U}) \cdot \nabla \mu_{eff} + \mathbf{f}_s \tag{2}$$

Where, U is the velocity of flow field; U_g represents the velocity on grid nodes; $p_d=p-\rho g\cdot x$ is the dynamic pressure instead of the total pressure by subtracting the hydrostatic component; g is the gravity acceleration vector; ρ is the mixture density with two phases (water and air) which is defined with VOF; the definition of effective dynamic viscosity is made with $\mu_{eff}=\rho(\upsilon+\upsilon_t)$, in which υ and υ_t are the kinematic viscosity and eddy viscosity respectively; here f_s represents the source term. In order to meet the closure requirement and solve RANS equations, the two-equation turbulence model k-ω SST [17] is employed, where the turbulent kinetic energy k and the turbulent dissipation rate ω are described as:

$$\frac{\partial}{\partial t}(\rho k) + \frac{\partial}{\partial x_i}(\rho k \mathrm{u}_i) = \frac{\partial}{\partial x_j}(\Gamma_k \frac{\partial k}{\partial x_j}) + \mathrm{G}_k - Y_k + S_k \tag{3}$$

$$\frac{\partial}{\partial t}(\rho \omega) + \frac{\partial}{\partial x_i}(\rho \omega \mathrm{u}_i) = \frac{\partial}{\partial x_j}(\Gamma_\omega \frac{\partial \omega}{\partial x_j}) + \mathrm{G}_\omega - Y_\omega + D_\omega + S_\omega \tag{4}$$

Where, Γ_k and Γ_ω are the effective diffusion coefficients for the turbulent kinetic energy k and the turbulent dissipation rate ω respectively, G_k and G_ω are turbulence generation terms for k and ω, Y_k and Y_ω are turbulent dissipation terms, Sk and S_ω are the source terms, D_ω is the cross-diffusion terms for ω.

naoe-FOAM-SJTU Solver

The two coupling solvers used in this paper employ the same in–house solver, naoe-FOAM-SJTU [18-20], to achieve the hydrodynamic prediction. Based on the open source CFD platform, this solver is designed for computing viscous flows of ships and ocean structures. It inherits the data structure and CFD libraries in OpenFOAM, such as FVM, RANS, VOF and PISO algorithm. The two-phase incompressible RANS equations are solved in this solver. The governing equations are discretized with Finite Volume Method (FVM) which is capable to handle arbitrary polyhedral cells. The interface between two phases is captured using a VOF method with bounded compression technique. The turbulence models of k–ω SST and $k-\varepsilon$ can be used for turbulence closure. The pressure-velocity coupling equations are solved by Pressure-Implicit with Splitting of Operations (PISO) algorithm.

Based on the above, a numerical tank system including wave generation and absorption module is built up, six-degree-of-freedom (6DOF) motion module is developed, and finally the mooring system module is added (Fig.1).

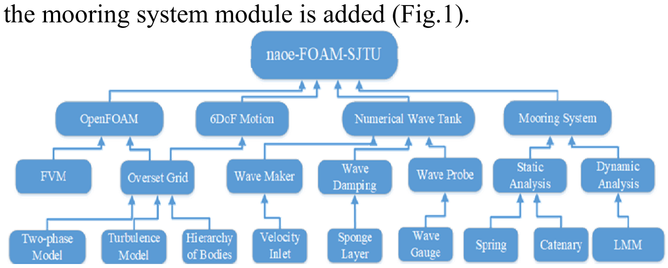

Fig.1 Frame Diagram of naoe-FOAM-SJTU solver

The wave generation system is able to use boundary inlet to generate first order regular waves and high order nonlinear waves, transient extreme waves and freak wave. To avoid wave reflection on the outlet or sidewall boundaries, the sponge layer is adopted for wave absorption. The mooring system module is built for hydrodynamic analysis of floating offshore structures which are moored in waters, such as Semi-submersible, TLP, Spar and FPSO. Several quasi static models including spring, catenary, piecewise extrapolation method as well as a dynamic model lumped mass method, are utilized for simulation of mooring lines. To solve 6DOF equations, two coordinate systems are used, which are the earth-fixed coordinate system and the body-fixed coordinate system. And both dynamic deformation mesh method and overset grid technique are employed to deal with the 6DOF issues. With these modules, naoe-FOAM-SJTU solver can be applied to the simulation of ship advancing, sea-keeping, superposition of complex motions, and hydrodynamics of floating platforms..

Unsteady Actuator Line Model

The FOWT-UALM-SJTU solver is developed by coupling the unsteady actuator line model (UALM) with in house code naoe-FOAM-SJTU, where the UALM is utilized to implement the aerodynamic prediction of FOWT.

The actuator line model (ALM) is an effective method to reduce computational cost by displacing the real blades surfaces with virtual actuator elements withstanding body forces, in which case there is no need to solve the blade geometry layer. When the ALM is applied to the simulation of the FOWTs, the velocity vector (U_M) induced by the motions of the floating platform is added into the velocity triangle (as shown in Fig.2), which will lead to complex interactions between the rotor and its wake. So the ALM needs to be modified to solve the unsteady problem caused by the dynamic motion responses of floating platform. The unsteady actuator line model considering the effect of six-degree-of-freedom motions is used in this paper.

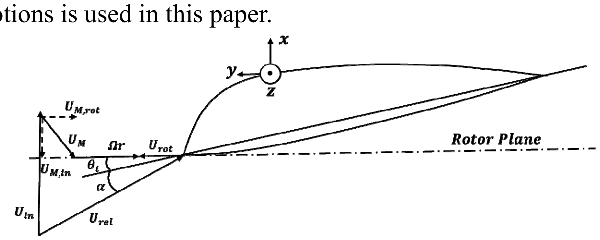

Fig.2 Cross-sectional airfoil element

In order to determine the aerodynamic forces acting on rotor blades, a blade element method combined with two-dimensional (2D) airfoil characteristics is used. Fig.2 shows a cross-sectional element at radius r which defines the airfoil in the xOy plane. The integral velocity vectors relationship is described as:

$$\mathbf{U}_{rel} = \mathbf{U}_{in} + \mathbf{\Omega} \times \mathbf{r} + \mathbf{U}_{rot} + \mathbf{U}_{M} \tag{5}$$

Where, $\mathbf{U_{in}}$ represents the inflow velocity vector, $\mathbf{U_{rot}}$ is the flow velocity induced by the rotating blade, $\mathbf{\Omega} \times \mathbf{r}$ is the speed of airfoil causes by the blades rotation, $\mathbf{U_M}$ is the the additional airfoil velocity vector induced by the motions of the floating platform. The magnitude of the local velocity relative to the rotating blade is given as:

$$\left|\mathbf{U_{rel}}\right| = \sqrt{(\mathbf{U_{in}} - \mathbf{U_{M,in}})^2 + (\mathbf{\Omega} \times \mathbf{r} - \mathbf{U_{rot}} + \mathbf{U_{M,rot}})^2} \tag{6}$$

And the aerodynamic lift and drag forces can be given by the following equation:

$$\mathbf{f} = (\mathbf{L}, \mathbf{D}) = \frac{\rho \left|U_{rel}\right|^2 cN_b}{2rd\theta dz}(C_L \mathbf{e}_L + C_D \mathbf{e}_D) \tag{7}$$

Where, c is the chord length of the airfoil, N_b is the total number of blades; C_L and C_D are the lift and drag coefficient respectively, e_L and e_D denote the unit vectors in the directions of the lift and the drag respectively. The lift and drag coefficient are determined from measured or computed 2D airfoil data which are corrected with 3D effects.

The aerodynamic lift and drag forces are acting as body forces in the flow field after smooth treatment to avoid singular behavior.

$$\mathbf{f}_\varepsilon = \mathbf{f} \otimes \eta_\varepsilon \quad , \quad \eta_\varepsilon(d) = \frac{1}{\varepsilon^3 \pi^{3/2}} \mathrm{e}^{-\left(d_i/\varepsilon\right)^2} \tag{8}$$

Here, d_i is the distance between the measured point in flow field and the actuator points on the rotor. ε is a constant width parameter to adjust the strength of regularization function, and the parameter ε is suggested to be determined according to the length of grid near turbine blades or the chord length of airfoil [21]. And the body force added onto the right side of the momentum equations as a source term can be written as:

$$\mathbf{f}_\varepsilon(x, y, z, t) = \sum_{i=1}^{N} \mathbf{f}(x_i, y_i, z_i, t) \frac{1}{\varepsilon^3 \pi^{3/2}} \mathrm{e}^{-\left(d_i/\varepsilon\right)^2} \tag{9}$$

Then the UALM is programmed as a C++ class based on the OpenFOAM. And the body force is added as a source term f_ε on the right side of the momentum equations (Eq.2):

$$\frac{\partial(\rho\mathbf{U})}{\partial t} + \nabla \cdot (\rho(\mathbf{U} - \mathbf{U}_g))\mathbf{U} = -\nabla p_d - \mathbf{g} \cdot \mathbf{x} \nabla \rho + \nabla \cdot (\mu_{eff} \nabla \mathbf{U}) + (\nabla \mathbf{U}) \cdot \nabla \mu_{eff} + \mathbf{f}_s + \mathbf{f}_\varepsilon \tag{10}$$

Overset Grid Technique

The other method used in this paper is the direct simulation with naoe-FOAM-os-SJTU solver. For direct simulation of large-amplitude-motion and complicated motions with a hierarchy of bodies, the overset grid technique is employed.

Using overset grid technique, the separated overlapping grids for each part with independent motion are allowed, which makes it competitive in simulations of large amplitude motion problems. And the connection among each grid system is built up with interpolation at appropriate cells or points using DCI (domain connectivity information) which is produced by SUGGAR++ [22-23]. There are four main steps when using DCI in the overset grid technique: (1) to mark the hole cells which are located outside the simulation domain or of no interest, and exclude them from computation. (2) to seek for donor grids. Fig.3 shows series of cells around hole cells named fringe cells, and for each fringe cell there are several donor cells providing information from the donor grids, so the second step is to seek for the donor grids of each fringe cell and provide information from the donor grids. (3) to obtain the value of a variable ϕ of the fringe cell by interpolation using the following equation from the donor cells find in the second step.

$$\phi_I = \sum_{i=1}^{n} \omega_i \cdot \phi_i \tag{11}$$

Where ϕ_I is the value of a variable ϕ of the fringe cell, ϕ_i is the value for the *ith* donor cell, ω_i is the weight coefficient, which is dimensionless and follows the condition shown in Eq.12:

$$\sum_{i=1}^{n} \omega_i = 1 \tag{12}$$

(4) to optimize the overlapping area and improve the accuracy of interpolation.

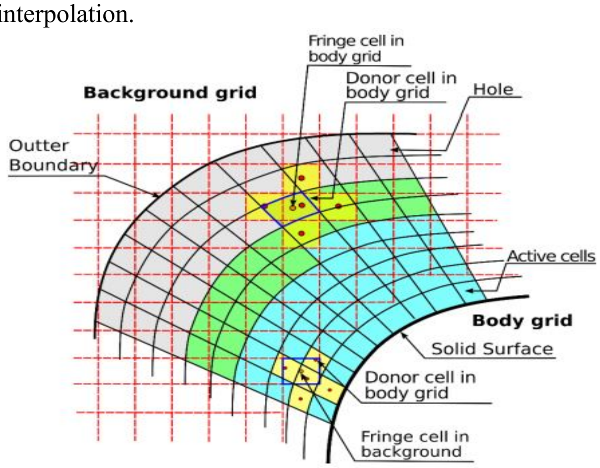

Fig. 3 Diagram of overset grid

DISCRIPTION OF GEOMETRY MODEL

In the present simulation work, a semi-submersible floating offshore wind turbine (FOWT) system, Phase II of OC4 project [24], is adopted. The FOWT contains several main parts: a wind turbine (the NREL-5MW baseline wind turbine), a tower supporting the turbine, the supporting floating platform (semi-submersible platform), and the mooring system. Fig.4 shows the sketch of this FOWT system, and Table.1 lists the basic properties.

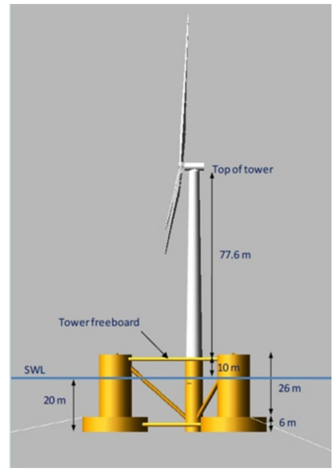

Fig.4 Phase II of OC4 Floating Offshore Wind Turbine System

Table.1 Specification of the Phase II of OC4 FOWT System

Rotor Orientation, Configuration	Upwind, 3 Blades
Rotor, Hub Diameter	126 m, 3 m
Hub Height	90 m
Rotor Mass	110,000 kg
Nacelle Mass	240,000 kg
Tower Mass	347,460 kg
Coordinate Location of CM (rotor, nacelle and tower)	(-0.2 m, 0.0 m, 64.0 m)
Total draft of platform	20m
Platform Mass	1.347E7 kg
Coordinate Location of CM (platform)	(0.0 m, 0.0 m, -13.46 m)
Number of Mooring Lines	3
Angle Between Adjacent Lines	120°
Depth to Anchors/Fairleads Below SWL	200m, 14m
Radius to Anchors/Fairleads from Platform Centerline	837.6m, 40.868m
Unstretched Mooring Line Length	835.5m
Mooring Line Diameter	0.0766m
Equivalent Extensional Stiffness	7.536E+8N
Equivalent Mass Density/ in water	113.35kg/m, 108.63kg/m

Table.2 Structural Properties of the FOWT System

Structural mass	1.407E7kg
CM location below SWL	9.9376m
Total structure roll inertia about CM	1.1E10 kg*m^2
Total structure pitch inertia about CM	1.1E10 kg*m^2
Total structure yaw inertia about CM	1.226E10 kg*m^2

The wind turbine in Phase II of OC4 FOWT system is NREL-5MW baseline line wind turbine, which is a conventional three-bladed, upwind, variable-speed and blade-pitch-to-feather controlled wind turbine. The floating support platform is a semi-submersible floating system which consists of a main column attached to the tower, three offset columns covering significant portion of buoyancy, a couple of smaller diameter pontoons and cross braces to link the main column and offset columns and to strengthen the structure. The semi-submersible floating system for Phase Ⅱ of OC4 is moored with three catenary lines spread symmetrically about the platform Z-axis..

RESULTS AND DISCUSSIONS

Comparison for Computational Efficiency

The fully coupled aero-hydrodynamic simulations of Phase II of OC4 FOWT system are conducted using the naoe-FOAM-os-SJTU solver and the FOWT-UALM-SJTU solver respectively. As introduced above, since the actual blades are represented with actuator elements, a great number of cells around blades are saved, which helps a lot to improve the computational efficiency of FOWT-UALM-SJTU. In this paper, the simulations conducted with two different solvers shared same background mesh and same grid structure for floating platform. In simulation with FOWT-UALM-SJTU, a refined region covered the rotating turbine blades with three levels refinement is provided in the background mesh system, while a well refined mesh system with 8 levels of boundary layers near the blades surface is required for more accurate simulations with naoe-FOAM-os-SJTU solver. The total number of cells in the simulation with FOWT-UALM-SJTU is 3.5M, while the number of mesh is about 7.3M in the naoe-FOAM-os-SJTU simulation.

Table.3 Computational Efficiency Comparison

Solver name	FOWT-UALM-SJTU	naoe-FOAM-os-SJTU
Number of cells	3.5M	7.3M
Time consumption for each time step	20s	56s

In two simulation cases, all the initial conditions and boundary conditions are the same. And both simulations are running in parallel with 40 processors. Table.3 lists the mesh numbers and time consumptions in two simulation cases. The number of cells in the naoe-FOAM-SJTU simulation is more than twice of that in the FOWT-UALM-SJTU simulation, which is necessary for direct CFD computation of the turbine blades. And it's very impressive that time consumption in the simulation using FOWT-UALM-SJTU solver is just 1/3 of that in the direct simulation with naoe-FOAM-os-SJTU solver.

Dynamic Responses of the FOWT System

With the coupled simulations, both dynamic loads and motions are gained. Both simulations are conducted under the same environmental conditions: the inlet wind speed is 11m/s and the rotor rotating speed is 12.1rpm, the wave length is 146m and wave height is 4m, in which case the rotating period of the turbine rotor is 5s, and the wave period is 10s. Fig.5 shows the time history of aerodynamic thrust of turbine rotor in two simulations. Both curve show an oscillating regularity with the same period as wave, which is caused by the oscillating motion of the platform. However, significant cyclic variation with higher frequency is observed on the green curve. This variation results from the tower-shadow effects which not considered in the simulation with FOWT-UALM-SJTU solver, and the period of this variation equals to 1/3 of the rotating period of a three-bladed rotor. It's also obvious that the aerodynamic thrust of turbine is over predicted with the FOWT-UALM-SJTU solver than that with naoe-FOAM-SJTU solver.

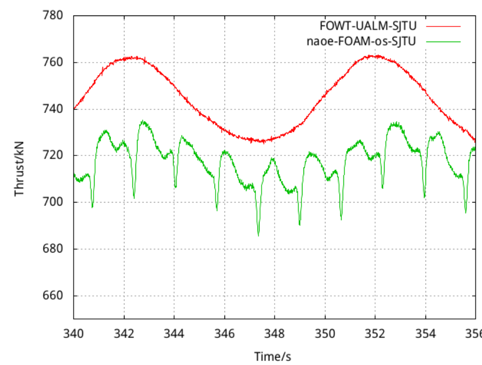

Fig.5 Aerodynamic Thrust

Fig.6 shows the dynamic surge and pitch motions of the supporting platform, which are most significant in the simulations. During the time period (340s~356s), the platform has reached the steady state which means that the platform surges/pitches around an equilibrium position. The periodic oscillation of both surge and pitch motions are resulted from the cyclic wave loads, while the deviation of the equilibrium position from the initial one arises mainly from aerodynamic forces. Because of the underestimation of the aerodynamic forces on the turbine with naoe-FOAM-os-SJTU solver, the equilibrium position of the green curve is lower than that of the red curve in Fig.6 (a).

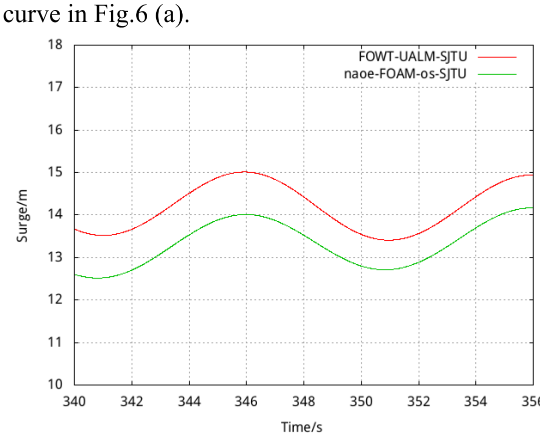

(a) Surge

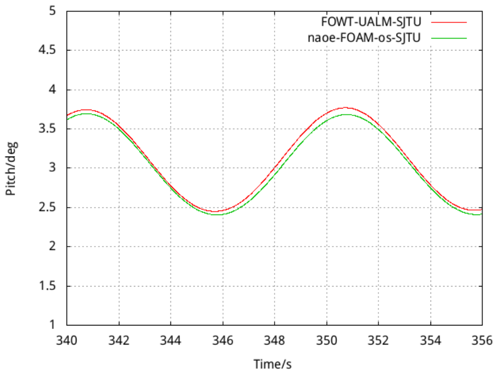

(b) Pitch

Fig.6 Dynamic Motions of the Supporting Platform

Detailed Flow Analysis

The direct simulation with naoe-FOAM-os-SJTU provides more detailed flow information near the blades surface, for example the pressure and velocity distributions around the blades cross section shown in Fig.7 and Fig.8, and also the pressure distribution on the blade surface shown in Fig.9.

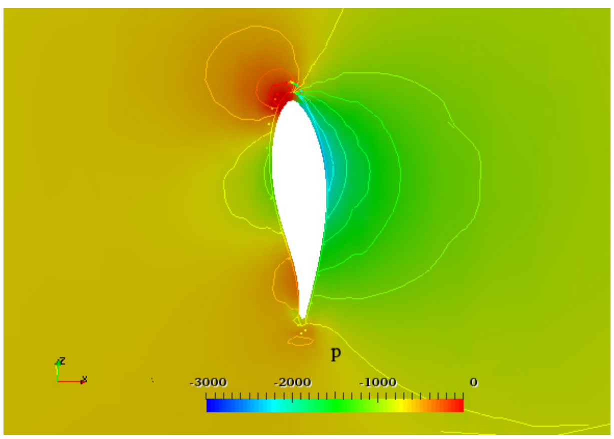

Fig.7 Pressure Distribution on the cross section with r/R=60% at t=352.7s

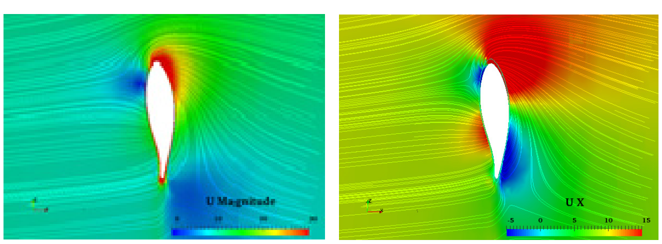

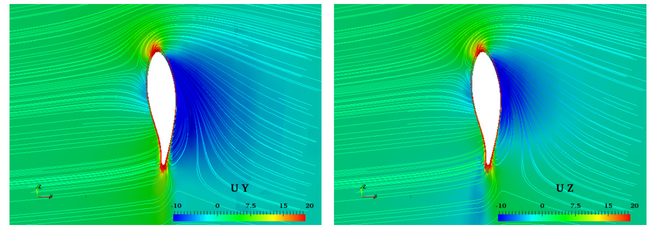

Fig.8 Velocity Distribution on the cross section with r/R=60% at t=352.7s

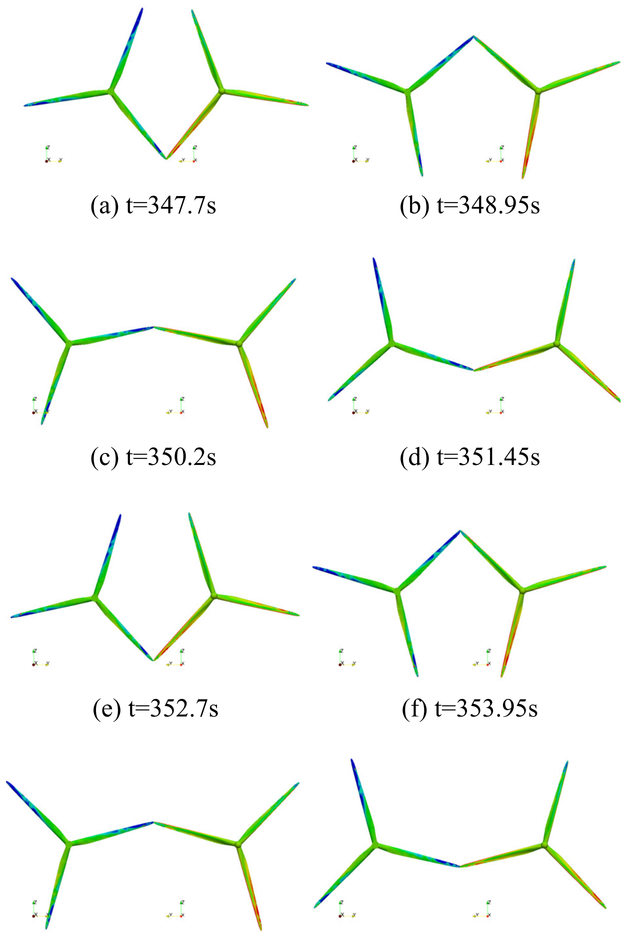

(a) t=347.7s (b) t=348.95s

(c) t=350.2s (d) t=351.45s

(e) t=352.7s (f) t=353.95s

(g) t=355.2s (h) t=356.45s

Fig.9 Variation of Pressure Distribution on the Blades Surface during one Wave Period

In the direct simulation with naoe-FOAM-os-SJTU, the dynamic loads are computed with pressure integral on the structure surface. And the pressure distribution on the blades surface indicates the variation of the aerodynamic loads.

CONCLUSIONS

Fully coupled aero-hydrodynamic simulations of the Phase II of OC4 floating offshore wind turbine system are conducted with in house solve FOWT-UALM-SJTU and naoe-FOAM-os-SJTU respectively. Both solvers utilize the same hydrodynamic simulation solve, the in house code naoe-FOAM-SJTU. In FOWT-UALM-SJTU, the turbine blades are simplified as series of actuator elements with body forces, in which case the computational efficiency is significantly improved. On the other side, refined mesh with boundary layer is generated for direct simulation of turbine blades for simulations with naoe-FOAM-os-SJTU, which increases the total number of cells and decreases the computational efficiency. But the direct simulations provide more detailed flow information for further deeply mechanism analysis. In addition, the dynamic forces and motions obtained from the two simulations differ little with each other, where the FOWT-UALM-SJTU solver shows little over prediction on aerodynamic forces and thus results in overvalue of the surge motions.

ACKNOWLEDGMENTS

This work is supported by the National Natural Science Foundation of China (51490675, 11432009, 51579145), Chang Jiang Scholars Program (T2014099), Shanghai Excellent Academic Leaders Program (17XD1402300), Program for Professor of Special Appointment (Eastern Scholar) at Shanghai Institutions of Higher Learning (2013022), Innovative Special Project of Numerical Tank of Ministry of Industry and Information Technology of China (2016-23/09) and Lloyd's Register Foundation for doctoral student, to which the authors are most grateful.

REFERENCES

[1] Archer CL, Jacobson MZ, 2005. Evaluation of global wind power. Journal of Geophysical Research, 110 (D12): 12110.

[2] Skaare B, Nielsen FG, Hanson TD, 2015. Analysis of measurements and simulations from the Hywind Demo floating wind turbine. Wind Energy, 18(6): 1105-1122.

[3] BBC, 2015. Floating wind farm to be installed off Peterhead. Available from: http://www.bbc.co.uk/news/uk-scotland-scotland-business-34694463.

[4] Luo N, Garcés JLP, Seguí YV, Zapateiro M, 2012. Dynamic load mitigation for floating offshore wind turbines supported by structures with mooring lines. àrees temàtiques de la upc::energies::energia eòlica.

[5] Viselli AM, Goupee AJ, Dagher HJ, 2015. Model test of a 1: 8-scale floating wind turbine offshore in the gulf of maine. Journal of Offshore Mechanics and Arctic Engineering, 137(4): 041901.

[6] Koo BJ， Goupee AJ， Kimball RW， 2014. Model tests for a floating wind turbine on three different floaters. Journal of Offshore Mechanics and Arctic Engineering， 136(2): 020907.

[7] Sandner F， Amann F， Azcona J，2015. Model building and scaled testing of 5MW and 10MW semi-submersible floating wind turbines. EERA DeepWind 2015 Conference ,Trondheim， Norway.

[8] Jonkman JM, 2009(a). Dynamics of offshore floating wind turbines—model development and verification. Wind energy, 12(5): 459-492.

[9] Cordle A, 2010. State-of-the-art in design tools for floating offshore wind turbines. Deliverable Report Under (SES6), UpWind project, Bristol, UK, Contract.

[10] Sebastian T, Lackner MA, 2013. Characterization of the unsteady aerodynamics of offshore floating wind turbines. Wind Energy, 16(3): 339-352.

[11] Tran TT, Dong HK, 2015(a). The aerodynamic interference effects of a floating offshore wind turbine experiencing platform pitching and yawing motions. Indian Journal of Thoracic and Cardiovascular Surgery, 29 (2): 549–561.

[12] Tran TT, Kim DH, 2016(a). A CFD study into the influence of unsteady aerodynamic interference on wind turbine surge motion. Renewable Energy, 90: 204–228.

[13] Tran TT, Kim DH, 2016(b). Fully coupled aero-hydrodynamic analysis of a semi-submersible FOWT using a dynamic fl uid body interaction approach. Renewable. Energy, vol. 92, pp. 244–261, 2016.

[14] Liu Y, Xiao Q, Incecik A, Incecik A, Peyrard C, Wan DC, 2017. Establishing a fully coupled CFD analysis tool for floating offshore wind turbines. Renewable Energy, 112: 280-301.

[15] Li PF, Cheng P, Wan DC, 2015. Numerical simulations of wake flows of floating offshore wind turbines by unsteady actuator line model. Proceedings of the 9th International Workshop on Ship and Marine Hydrodynamics, Glasgow, UK, 26 - 28 August.

[16] Karimirad M, Moan T, 2012. A simplified method for coupled analysis of floating offshore wind turbines. Marine Structures, 27(1): 45-63.

[17] Menter FR, 1994. Two-equation eddy-viscosity turbulence models for engineering applications. AIAA journal, 32(8): 1598-1605.

[18] Zhirong Shen and Decheng Wan, An Irregular Wave Generating Approach Based on naoe-FOAM-SJTU Solver, China Ocean Engineering, 2016, 30(2): 177-192.

[19] Hongjian Cao, Decheng Wan, Development of Multidirectional Nonlinear Numerical Wave Tank by naoe-FOAM-SJTU Solver, International Journal of Ocean System Engineering, Vol. 4, No. 1, 2014, pp. 52-59.

[20] Zhirong Shen and Decheng Wan, RANS Computations of Added Resistance and Motions of Ship in Head Waves, International Journal of Offshore and Polar Engineering, 2013, Vol. 23, No. 4, pp. 263-271.
[21] Sørensen JN, Shen WZ, 2002. Numerical modeling of wind turbine wakes. Journal of Fluid Engineering, 124: 393–99.
[22] Noack, RW, 2005. SUGGAR: a general capability for moving body overset grid assembly. In: Proceedings of the 17th AIAA Computational Fluid Dynamics Conference, American Institute of Aeronautics and Astronautics, Toronto, Ontario, Canada.
[23] Carrica P M, Huang J, Noack R, 2010. Large-scale DES computations of the forward speed diffraction and pitch and heave problems for a surface combatant. Computers & Fluids, 39(7): 1095-1111.
[24] Robertson A, Jonkman J, Masciola M, 2012. Definition of the Semisubmersible Floating System for Phase II of OC4. Offshore Code Comparison Collaboration Continuation (OC4) for IEA Task, 30.

